Effects of Alkyl-Group Substitution on the Proton-Transfer Barriers in Ammonium and Hydroxylammonium Nitrate Salts†

Saman Alavi and Donald L. Thompson*

Department of Chemistry, Oklahoma State University, Stillwater, Oklahoma 74078

Received: February 27, 2004; In Final Form: April 29, 2004

The effects of alkyl (CH_3 and C_2H_5) substitutions for hydrogen on the proton-transfer barriers in ammonium nitrate (AN) and hydroxylammonium nitrate (HAN) are studied by using ab initio electronic structure calculations. The optimized hydrogen-bonded neutral-pair structures and the ion-pair transition states for proton transfer are determined at the B3LYP/6-311++G(d,p) level. Zero-point energies, basis set superposition corrections, and single-point MP2 calculations on the optimized structures are applied to obtain binding energies for these hydrogen-bonded molecules. The alkyl substituents strengthen the hydrogen bonding in both the neutral- and ion-pair complexes, but the ion-pair forms are stabilized to a greater extent, which results in a decrease in the barrier to proton transfer and exchange. The energy barrier to proton transfer in AN is 8.1 kcal/mol, whereas in methylammonium (MeA), ethylammonium (EtA), and dimethylammonium (diMeA) nitrate this barrier decreases to 4.1, 3.7, and 1.4 kcal/mol, respectively. The alkyl substitution reduces the proton-transfer barrier, and the dialkyl substitution reduces it even further. A similar trend holds for HAN and methylhydroxylammonium nitrate (MeHAN); the barrier to proton transfer from the most stable neutral-pair HAN to the lowest-energy ion-pair configuration is 13.6 kcal/mol, whereas this barrier decreases to 9.5 kcal/mol in the corresponding MeHAN complex. The effect of the alkyl substitutions on the basicity and strength of hydrogen bonds in the complex is discussed.

I. Introduction

Hydrogen bonding and proton transfer can play critical roles in determining the structure and chemistry of molecules and materials. Perhaps the best known cases are in biochemistry, where hydrogen bonds determine critical structural features of proteins and nucleic acids.[1,2] Proton transfer is involved in many cellular processes such as trans-membrane transport in proton-conducting membrane proteins[3−5] and proton pumping in cytochrome *c* oxidase.[6,7] Intermolecular hydrogen bonding in molecular solids can also cause the formation of highly ordered crystal structures. This ordering can significantly influence the physical properties and chemical reactivity of these materials in response to heat and mechanical shock, which has practical ramifications on energetic materials' design.[8] Proton transfer and the effect of hydrogen bonding are important in ammonium salts, the most conspicuous illustration being the conversion of ion pairs in the condensed phase to neutral pairs upon sublimation or evaporation.[9−11] The decomposition of some hydrogen-bonded energetic materials from the solid phase may be initiated by a proton-transfer reaction.[12] Thus, there is considerable motivation to develop a better understanding of proton transfer and hydrogen bonding.

We have been investigating proton transfer in ammonium and substituted ammonium salts by using quantum chemistry calculations to determine equilibrium and transition-state energies and geometries in isolated molecules and clusters. Recently, we reported studies of ammonium nitrate (AN),[11] ammonium dinitramide (ADN),[13] and hydroxylammonium nitrate (HAN).[14] We continue this series with computational studies of the effects of alkyl (methyl and ethyl) substitutions on ammonia and hydroxylammonia with respect to proton transfer with nitric acid; specifically, we have investigated gas-phase complexes composed of CH_3NH_2, $C_2H_5NH_2$, $(CH_3)_2NH$, and $CH_3N(H)$-OH and the nitric acid molecule. We compare these results with those for AN and HAN reported earlier.[11,14] Although our focus is on nitrate salts of amines, we note that the proton-transfer process in these ion-pair/neutral-pair complexes is typical of those that occur in amino acids such as lysine.[15,16]

In the gas phase, many acid (HA) and base (:B) pairs form neutral-pair hydrogen-bonded complexes [A−H···B] in which the hydrogen is attached to the acid. Except for complexes of very strong bases, for example, $(CH_3)_3N$, and acids, such as HI, experiments show, for single acid−base gas-phase molecules, that the energy gained from the electrostatic interactions of A^- and $H-B^+$ in the proton transfer is not sufficient to compensate for the A−H bond dissociation. Therefore, the ion-pair [A^-···$H-B^+$] complex will be unstable compared to [A−H···B]. In molecules where the base :B has at least one hydrogen atom attached to the electronegative central atom, as in the case of :NH_3, primary amines :NH_2R, and secondary amines :NHR_2, the proton-transfer complex [A^-···$H-B^+$] is actually the saddle-point structure on the potential energy surface for double proton transfer between the acid and base.[9,11,14]

In our earlier work, the barriers to proton transfer from the stable neutral-pair forms of AN and HAN to the ion-pair hydrogen-bonded saddle points were calculated to be 8.1 and 13.6 kcal/mol, respectively, at the B3LYP/6-311++G(d,p) level of theory.[11,14] The ion-pair saddle point is a transition state for the double proton-transfer reaction between ammonia and nitric acid in AN and between hydroxylammonia and nitric acid in HAN. Factors that stabilize the ionic transition state for a [A^-···$H-B^+$] complex lower the barrier to proton transfer.

Effects of methyl group substitution for hydrogen on proton transfer between imines, amine oxides, and phosphine oxides with acid halides have been studied,[17,18] and a theoretical

† Part of the "Gert D. Billing Memorial Issue".

* Corresponding author. E-mail: dlt@okstate.edu.

10.1021/jp040189r CCC: $27.50
Published on Web 06/08/2004

criterion was developed to determine which of these complexes will have stable ion-pair forms in the gas phase. An extensive series of experimental and theoretical studies also have been carried out on ammonium and trimethylammonium halides to determine the percent ionic character of the hydrogen bonding between the $(CH_3)_3N$ and HX molecules.[19−23] High ionic character is observed for complexes of the strong acids HBr and HI. Latajka et al.[24] have theoretically determined the critical points of the potential energy surfaces for proton transfer between $(CH_3)_{3-n}H_nN$ ($n = 0$ to 3) and HBr and HI. They predict a shared proton arrangement in the HBr and methylated amine complexes, whereas HI forms stable ion-pair complexes.

In the present study, the effect of alkyl substitutions on hydrogen bonding in amine complexes with nitric acid is investigated. Alkyl substitutions on ammonia species increase their basicity and lower the proton-transfer barrier in their salts. This effect is quantitatively studied in this work. This is an extension of our theoretical studies on hydrogen bonding in gas-phase AN[11] and HAN[14] to gas-phase methyl, ethyl, and dimethylammonium nitrates and methylhydroxylammonium nitrate. Because we are interested in the possibility of double proton transfer between the acid and base, the studies are limited to doubly substituted amines where at least a single hydrogen remains attached to the basic amine nitrogen. The alkyl groups on the nitrogen atoms increase the basicity of the molecules and lower the proton-transfer energy barrier between the acid and base.

A summary of theoretical methods is given in section II. A method for calculating the basis set superposition error (BSSE) for ionic transition states is also presented in this section. The structures and energies of the various molecules are presented in section III, and an interpretation of these values in terms of the hydrogen bonding strength in the A⁻H···B complexes is given in section IV. A summary and the conclusions are given in section V.

II. Theoretical Methods

Calculations were made with the Gaussian 98 suite of programs.[25] The geometric optimization of the structures, energy, and normal-mode frequency calculations was done with density functional theory (DFT)[26,27] using the B3LYP hybrid Hartree−Fock nonlocal approach of Becke.[28] The diffuse 6-311++G(d,p) basis set is used throughout to model the long-range hydrogen bonding accurately. No geometric constraints were applied during the optimizations. DFT calculations are known to underestimate transition-state barriers for proton transfer in $H_2O^+H\cdots HOH$[29,30] and $H_3N^+H\cdots NH_3$;[31] however, by using single-point energy calculations at the MP2/6-311++G-(d,p)[32,33] level in DFT optimized structures, more accurate transition-state energies can be obtained. For other hydrogen-bonded complexes containing the ammonium ion, theoretical studies show that structures determined from optimizing stable molecules and transition states with DFT calculations correspond closely to MP2 optimized structures.[15,31] The accurate representation of optimized geometries by B3LYP/6-311++G(d,p) calculations also forms the basis of the G2M method.[34]

BSSEs[1,27,35,36] for the binding energies of the neutral-pair hydrogen-bonded molecules were estimated using the counterpoise method[37] along with corrections for the geometric relaxation of the fragments in the hydrogen-bonded molecule.[38] For the hydrogen-bonded neutral-pair complex, the binding energy with counterpoise corrections is calculated with reference to separated starting molecules. The binding energy $D_b^{CP}(AH;B)$ is given as

$$D_b^{CP}(AH;B) = E(AH\cdots B) - [E_B^{CP}(AH\cdots B) + E_{AH}^{CP}(AH\cdots B)] + [E_B(AH\cdots B) - E(B)] + [E_{AH}(AH\cdots B) - E(AH)] \quad (1)$$

where $E(AH\cdots B)$ is the energy of the neutral-pair acid−base complex, $E_X^{CP}(AH\cdots B)$ is the energy of fragment X of the complex with the counterpoise corrections for the molecular orbitals of the complementary fragment in the complex, $E_X(AH\cdots B)$ is the energy of fragment X with geometry identical to that observed in the complex, and $E(X)$ is the energy of the relaxed neutral species X in the gas phase. The geometrical distortions of nitric acid and the basic molecules in the neutral hydrogen-bonded complexes are small relative to those of the isolated species, thus the distortion energies in the BSSE will not be large.

For the formation of ion-pair hydrogen-bonded transition state complexes,

$$A{-}H + :B \rightarrow A^-\cdots H{-}B^+ \quad (2)$$

counterpoise corrections to the binding energy are more appropriately written with reference to the structures and energies of the ionic fragments, rather than the neutral species, as given in eq 1. In this case, the expression for the corrected binding energy is

$$D_b^{CP}(A^-;HB^+) = E(A^-\cdots HB^+) - [E_{HB^+}^{CP}(A^-\cdots HB^+) + E_{A^-}^{CP}(A^-\cdots HB^+)] + [E_{HB^+}(A^-\cdots HB^+) - E(HB^+)] + [E_{A^-}(A^-\cdots HB^+) - E(A^-)] \quad (3)$$

where $E(A^-\cdots HB^+)$ is the energy of the ion-pair complex, $E_X^{CP}(A^-\cdots HB^+)$ is the energy of fragment X of the complex with the counterpoise corrections for the molecular orbitals of the complementary fragment in the complex, and $E_X(A^-\cdots HB^+)$ is the energy of fragment X with geometry identical to that observed in the complex. The geometrical distortion energies in the hydrogen-bonded ion-pair complexes are calculated with reference to the structures of isolated ions, not neutral species. The structural distortions caused by hydrogen bonding in the ion-pair complexes are not considered to be large, relative to those of the isolated gas-phase ionic species, and as a result, the distortion energies in the BSSE will not be large.

It should be noted that when using eqs 1 and 3 to determine the BSSE we calculated the structural distortions of the fragments in each hydrogen-bonded complex with reference to closely related isolated molecules. Thus, the distortion energy of the ion-pair complexes is calculated relative to that of the isolated ions, and the distortion energy of the neutral-pair complexes is calculated relative to that of the isolated gas-phase neutral molecules. The distortion energies of the ion-pair complex calculated with reference to those of neutral molecules will be very large and do not properly reflect the nature of the BSSE correction.

By combining the expression in eq 3 with the ionization energies of H−A and :B,

$$A{-}H(g) + :B(g) \rightarrow A^-(g) + H{-}B^+(g) \quad (4)$$

$$\Delta E_{ion} = E[A^-(g)] + E[HB^+(g)] - E[A{-}H(g)] - E[:B(g)] \quad (5)$$

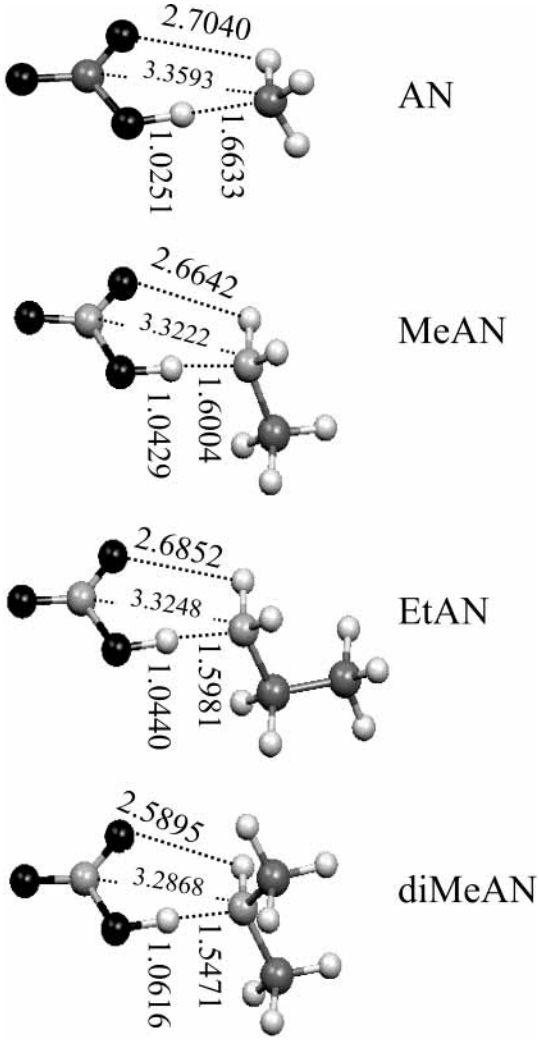

Figure 1. Structures of AN, MeAN, EtAN, and diMeAN optimized at the B3LYP/6-311++G(d,p) level. Bond lengths (Å) are given for atoms involved in hydrogen bonding. Alkyl substitution on ammonia strengthens hydrogen bonding.

we can derive the value for the binding energy with counterpoise corrections with HA and :B as the starting materials:

$$D_b^{CP}(AH;B) = D_b^{CP}(A^-;HB^+) - \Delta E_{ion} \qquad (6)$$

$D_b^{CP}(AH;B)$ is the binding energy of the ion-pair complex, starting from neutral, isolated gas-phase molecules. Note that the BSSE for the ion pair is correctly based on the structures of the isolated gas-phase ions. This quantity will be used as a measure of the binding strength of the fragments in the transition states. Equations 5 and 6 are general and can be used to determine the BSSE for neutral systems that react via ion-pair transition states. The basis sets chosen in this work are large and include diffuse functions, thus we do not expect the BSSE to be large.

III. Results

The lowest-energy neutral-pair configurations for gas-phase AN, methylammonium nitrate (MeAN), ethylammonium nitrate (EtAN), and dimethylammonium nitrate (diMeAN) molecules were determined by quantum chemical calculations at the B3LYP/6-311++G(d,p) level. The optimized structures of the molecules are shown in Figure 1 along with selected bond lengths. The most stable structures are those in which the ammonia or substituted amines are hydrogen bonded to nitric acid. The energies of the DFT-optimized geometry (with zero-point energies in parentheses) along with the corresponding MP2 energies calculated for the DFT geometries are given in Table 1.

TABLE 1: Absolute Energies (hartrees) of Various Molecules and Ions with the Corresponding Zero-Point Energy in Parentheses (kcal/mol) for DFT- and MP2-Level Calculations

molecule	E (ZPE)[a]	E[b]
NH_3	−56.582722 (21.5)	−56.415498
NH_4^+	−56.920362 (31.0)	−56.755675
HNO_3	−280.978606 (16.5)	−280.328150
NO_3^-	−280.457566 (8.7)	−279.800055
CH_3NH_2	−95.893889 (40.0)	−95.593873
$CH_3NH_3^+$	−96.249056 (49.7)	−95.950957
$C_2H_5NH_2$	−135.221527 (57.9)	−134.792518
$C_2H_5NH_3^+$	−135.582038 (67.4)	−135.153500
$(CH_3)_2NH$	−135.209633 (57.7)	−134.778725
$(CH_3)_2NH_2^+$	−135.576241 (67.6)	−135.147204
H_2NOH	−131.766887 (25.3)	−131.429207
H_3N^+OH	−132.086514 (34.1)	−131.751117
$H_2NO^+H_2$	−132.045514 (32.9)	−131.708489
CH_3NHOH	−171.087280 (42.9)	−170.618173
$CH_3N^+H_2OH$	−171.424368 (52.0)	−170.957273
$CH_3NHO^+H_2$	−171.378373 (49.9)	−170.905877
$NH_3\cdots HONO_2$	−337.584052 (39.8)	−336.766327
$NH_4^+\cdots NO_3^-$	−337.571194 (39.6)	−336.748645
$CH_3NH_2\cdots HONO_2$	−376.896791 (57.8)	−375.947000
$CH_3NH_3^+\cdots NO_3^-$	−376.890237 (58.2)	−375.936322
$C_2H_5NH_2\cdots HONO_2$	−416.224590 (75.6)	−415.145745
$C_2H_5NH_3^+\cdots NO_3^-$	−416.218636 (76.0)	−415.135483
$(CH_3)_2NH\cdots HONO_2$	−416.213136 (75.2)	−415.133771
$(CH_3)_2NH_2^+\cdots NO_3^-$	−416.210922 (76.1)	−415.127823
HAN (NO-bonded)	−412.768518 (43.4)	−411.780350
HAN (N-bonded)	−412.763644 (43.0)	−411.775878
HAN (O-bonded)	−412.760568 (43.0)	−411.773109
$HON^+H_3\cdots NO_3^-$	−412.746804 (43.5)	−411.756040
$H_2NO^+H_2\cdots NO_3^-$	−412.735282 (40.7)	−411.744710
MeHAN (NO-bonded)	−452.090469 (60.7)	−450.972118
MeHAN (N-bonded)	−452.085511 (60.4)	−450.967832
MeHAN (O-bonded)	−452.081438 (60.3)	−450.962694
MeHAN-ts (NO → N)	−452.075311 (61.3)	−450.954471
MeHAN-ts (O)	−452.056903 (58.3)	−450.934787

[a] Calculations at the B3LYP/6-311++G(d,p) level. [b] Calculations at the MP2/6-311++G(d,p)// B3LYP/6-311++G(d,p) level.

The implication of the values of the bond lengths given in Figure 1 is that the hydrogen bonds in alkyl-substituted molecules are stronger than those in AN. The lengths of the H···N and H···O hydrogen bonds decrease from 1.663 and 2.707 Å, respectively, in AN to 1.547 and 2.590 Å in diMeAN. The hydrogen-bond lengths in the methyl- and ethyl-substituted ammonium nitrates are between these values and differ from each other by only ∼1%.

The ion-pair transition states, designated as AN-ts, MeAN-ts, EtAN-ts, and diMeAN-ts, are composed of hydrogen-bonded alkylammonium and nitrate ions; these are shown in Figure 2. These structures are transition states for double proton transfer between the (alkyl) ammonia bases and nitric acid, detailed discussions of which are given in refs 9, 11, and 14. The energies of the separated ions and the gas-phase complexes are given in Table 1. In all cases, the hydrogen-bonded ion pairs are higher in energy than the neutral-pair structures shown in Figure 1. Of the four transition-state structures, charges are more localized in the AN-ts form, and as a result, hydrogen bonding is strongest in this structure. This trend for hydrogen-bond strength is opposite that observed in the neutral species. The H···O

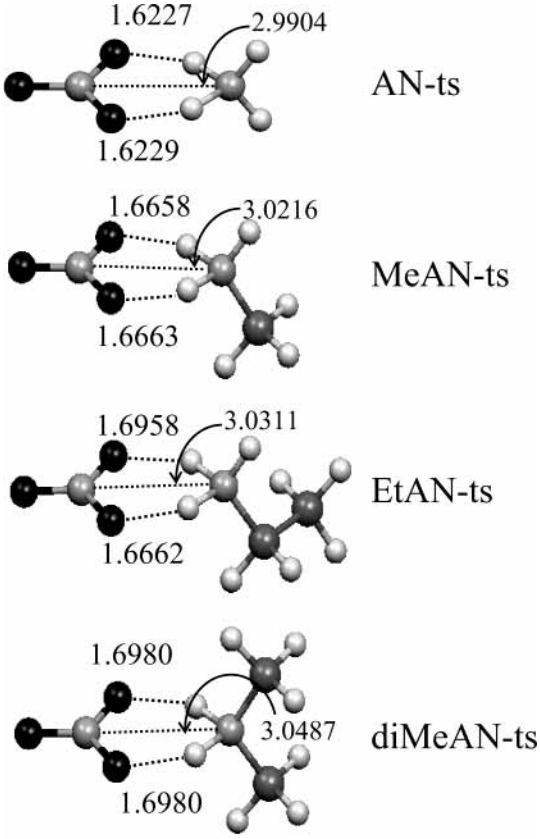

Figure 2. Structures of proton-transfer transition states AN-ts, MeAN-ts, EtAN-ts, and diMeAN-ts optimized at the B3LYP/6-311++G(d,p) level. Bond lengths (Å) are given for atoms involved in hydrogen bonding. Alkyl substitution on ammonia stabilizes the cation and weakens hydrogen bonding.

hydrogen bond is shortest in the AN-ts structure, 1.623 Å. It is 1.698 Å in diMeAN-ts.

The binding energies of the molecules and bonding strength of the transition states relative to those of ammonia or alkylamines and nitric acid are given in Table 2. The energies, D_b^{NCP}, which do not include zero-point energies and counterpoise corrections, are given for both the B3LYP/6-311++G(d,p) (see column 2) and the MP2/6-311++G(d,p)//B3LYP/6-311++G(d,p) (see column 5) levels of calculation in Table 2. In general, the MP2 binding energies of the molecular complexes are larger than the DFT values (by <1 kcal/mol), whereas the hydrogen-bonded ion-pair transition-state species have smaller MP2 binding energies compared to the DFT values (by 1 to 2 kcal/mol). It is generally known that for some hydrogen-bonding systems DFT methods may underestimate transition-state energy barriers.[31−33,39] The MP2 energies provide a check for consistency of the DFT results. The calculated values of the energy differences between neutral-pair and ion-pair complexes are 2 to 3 kcal/mol larger for the MP2 level compared to those computed by using DFT (Table 2).

Binding energies, D_0^{NCP}, for the same species, with the unscaled zero-point energies from normal-mode analyses but without the counterpoise corrections for the B3LYP/6-311++G(d,p) level, are given in column 3 of Table 2. The inclusion of zero-point energy decreases the binding energy by 1 to 2 kcal/mol.

Binding energies computed by using DFT, with counterpoise corrections, D_b^{CP}, for neutral-pair species evaluated according to eq 1, are given in column 4 of Table 2. The transition-state structures are naturally related to the ammonium and nitrate

TABLE 2: Binding Energies and Electrostatic Interaction Energies (kcal/mol) for Hydrogen-Bonded Ammonium Salts

molecule	D_b^{NCP} [a,b]	D_0^{NCP} [a,b,c]	D_b^{CP} [a,d]	D_b^{NCP} [b,e]	E_{coul} [a,f]
$NH_3\cdots HNO_3$	14.3	12.4	13.1	14.2	−16.1
$NH_4^+\cdots NO_3^-$	6.2	4.5	5.5	3.1	−92.8
$CH_3NH_2\cdots HNO_3$	15.2	13.9	14.1	15.7	−17.3
$CH_3NH_3^+\cdots NO_3^-$	11.1	9.5	10.5	9.0	−92.1
$C_2H_5NH_2\cdots HNO_3$	15.3	14.1	14.2	15.7	−16.9
$C_2H_5NH_3^+\cdots NO_3^-$	11.6	10.0	10.9	9.3	−63.1
$(CH_3)_2NH\cdots HNO_3$	15.6	14.6	14.4	16.9	−19.6
$(CH_3)_2NH_2^+\cdots NO_3^-$	14.2	12.3	13.8	13.1	−71.4
HAN (NO-bonded)	14.4	12.7	13.2	14.4	−11.1
HAN (N-bonded)	11.4	10.1	10.4	11.6	−6.7
HAN (O-bonded)	9.4	8.2	8.5	9.9	−13.1
HAN-ts (NO→N)	0.8	−0.9	−0.2	−0.8	−113.1
HAN-ts (O)	−6.4	−5.3	−7.7	−7.9	−81.5
MeHAN (NO-bonded)	15.4	14.1	14.3	16.2	−13.2
MeHAN (N-bonded)	12.3	11.3	11.4	13.5	−9.2
MeHAN (O-bonded)	9.8	8.6	9.0	10.3	−14.2
MeHAN-ts (NO → N)	5.9	4.0	4.8	5.1	−110.6
MeHAN-ts (O)	−5.6	−4.5	−7.0	−7.2	−82.8

[a] Calculations at the B3LYP/6-311++G(d,p) level. [b] Counterpoise corrections are not included. [c] Includes zero-point energies. [d] Includes counterpoise corrections. [e] Calculations at the MP2/6-311++G(d,p)//B3LYP/6-311++G(d,p) level. [f] Calculated from eq 7 using charges from natural population analysis.

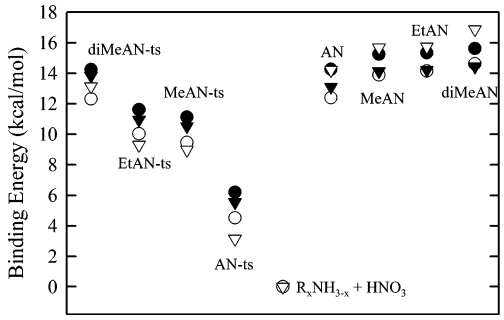

Figure 3. Binding energies D_b^{NCP} (●) from DFT calculations, and D_0^{NCP}(○), D_b^{CP}(▼), and D_b^{NCP}(▽) from MP2 calculations of AN and alkyl-substituted AN molecules along with the proton-transfer transition states. The structures of the molecules and transition states are given in Figures 1 and 2. Alkyl substitutions on ammonia stabilize both the neutral-pair and the ion-pair forms of the hydrogen-bonded complexes.

ions, and eqs 3 and 6 are used to calculate their effective binding energies. For the neutral pairs, the BSSE corrections are generally between 1 and 1.5 kcal/mol, whereas these corrections for ion-pair transition states are <1 kcal/mol. The hydrogen bonds are weaker and the electrons are more localized in the ion-pair transition states, and as a result, the BSSE is smaller for the ion pairs. The binding energies for AN and the alkylammonium nitrate molecules illustrated in Figure 3 show the effect of the alkyl groups on increasing the binding energy of the neutral molecules and the ionic transition states. The stabilizing effect is greater for the transition states, so the energy difference between the neutral and ionic forms of the alkylated molecules decreases relative to that of ammonium nitrate. The last column in Table 2 lists the electrostatic interaction energies in the complexes, which will be discussed in section IV.

Gas-phase structures and energies of HAN and MeHAN were also calculated. The optimized gas-phase structures of these molecules obtained by using DFT are hydrogen-bonded neutral-pair species; these are shown in Figure 4 with selected bond lengths. Three stable hydrogen-bonded structures previously reported[14] are also shown in Figure 4; these are labeled HAN−NO, HAN−N, and HAN−O. The HAN−NO structure has the

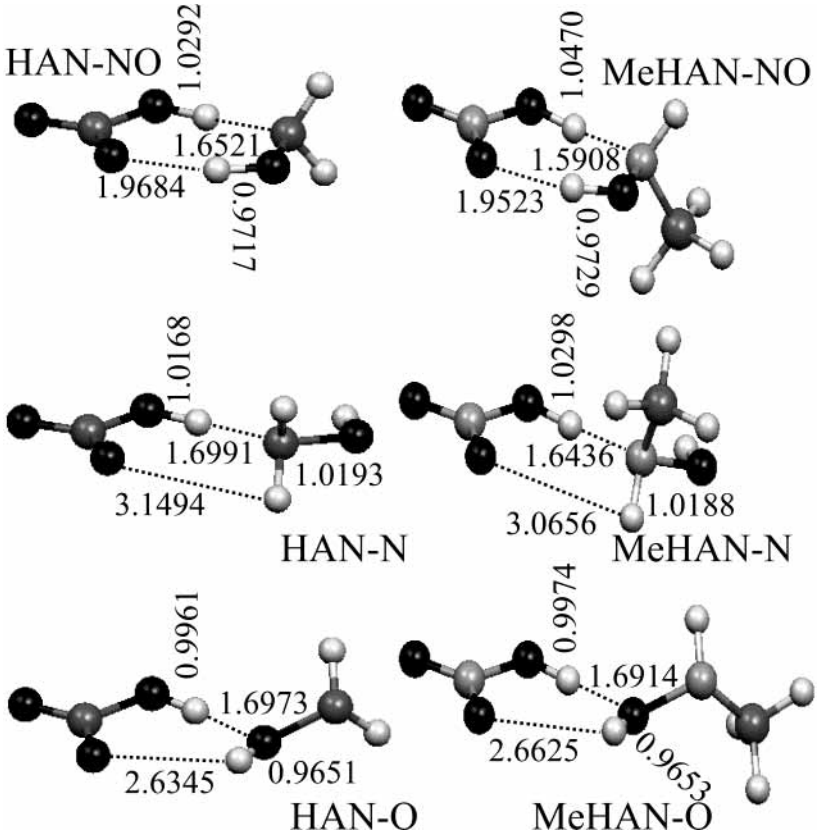

Figure 4. Optimized structures for three hydrogen-bonded configurations of HAN and MeHAN. Bond lengths (Å) are given for atoms involved in hydrogen bonding. Methyl substitution on hydroxylammonia strengthens the hydrogen bonds in the NO- and N-bonded configurations. In the O-bonded configuration, the methyl group is not attached to the hydrogen-bonded oxygen atom, thus its effect on the strength of the hydrogen bonding is diminished.

largest binding energy (as discussed below) with both the nitrogen and the oxygen of the hydroxylamine molecule participating in hydrogen bonding. The hydroxylamine nitrogen is the proton acceptor from the nitric acid OH group, and the oxygen is the proton donor to another nitric acid O atom. In the HAN−N structure, the hydroxylamine N atom is the proton acceptor, and the nitric acid OH is the proton donor. The NH_2 H atoms interact electrostatically with a nitric acid O atom and are symmetrically oriented with respect to that oxygen atom; the H−O distances are too large (3.15 Å) to be described as hydrogen bonds. There are two hydrogen bonds in the HAN−O structure; they involve the OH on the hydroxylamine and the OH on the nitric acid molecule. The MeHAN complexes have analogous structures; these are also shown in Figure 4. The hydrogen bonds in the MeHAN species are stronger than those in the analogous HAN species on the basis of comparisons of the hydrogen-bond lengths. The DFT (zero-point energies are given in parentheses) and MP2 energies with the DFT geometry of the separate molecules and the corresponding energies of the hydrogen-bonded complexes are given in Table 1.

HAN and MeHAN each have two ion-pair transition-state structures for proton exchange; these are shown in Figure 5 along with selected bond lengths. These are labeled as HAN-ts(NO → N), HAN-ts(O), MeHAN-ts(NO → N), and MeHAN-ts(O). Proton transfer through the (NO → N) transition state converts the HAN or MeHAN complex from the NO-bonded form to the N-bonded form. Additional details of this proton-exchange reaction are given in ref 14. On the basis of the shorter hydrogen-bond lengths, the hydrogen bonds in the HAN and MeHAN ion-pair transition states are stronger than those in the neutral analogues of Figure 4.

The various binding energies of the HAN and MeHAN species are given in Table 2. The observations made in the preceding paragraphs for the comparison of the AN and alkylated AN species hold for these cases as well. The MeHAN molecules form stronger hydrogen bonds in the neutral-pair structures, whereas the HAN forms have shorter bond lengths and stronger hydrogen bonds in the ion-pair transition states.

Similar to the AN and alkylated AN complexes, the binding energies (Table 2) from MP2 calculations are larger than the DFT results for HAN and MeHAN complexes but smaller for the HAN-ts and MeHAN-ts structures; therefore, the energy differences between the equilibrium structures and transition states from the MP2 calculations are ∼2 kcal/mol greater than those predicted from the DFT calculations, including the fact that the zero-point energy decreases the binding energy in all cases. Counterpoise corrections also lower the binding energies, with the effect being greater for the neutral-pair transition states than for the ion-pair transition states. The binding energies of the HAN and MeHAN molecules and transition states are shown in Figure 6. The neutral-pair and ion-pair forms are both stabilized by the methyl substituent; however, the ion-pair is stabilized to a greater extent.

IV. Effect of Alkyl Groups on Binding-Energies

The effects of electron-donating alkyl groups on the binding energy and the hydrogen-bond lengths of the A−H···B and A^-···H−B^+ complexes were discussed in section III. It was observed that the alkyl-substituted ammonia groups stabilize the A−H···B complexes relative to what was observed in the case of the unsubstituted ammonia. This can be seen by comparing the values of the binding energies of the A−H···B

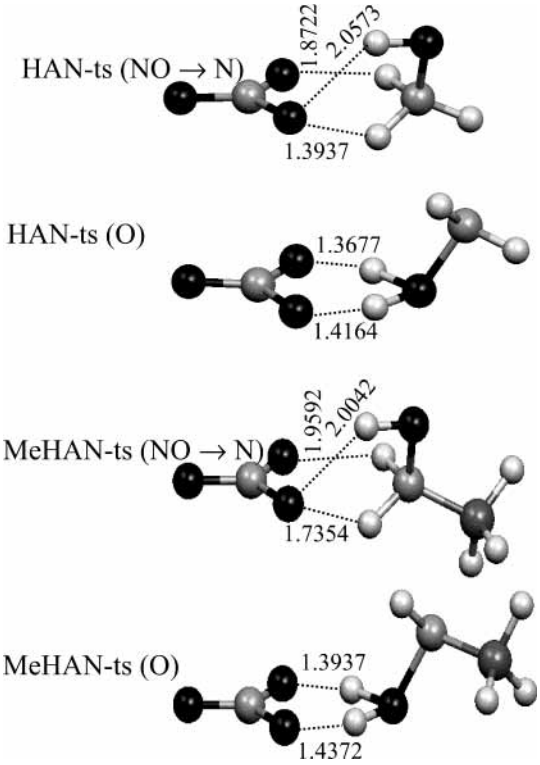

Figure 5. Structures of proton-transfer transition states HAN-ts (NO→N), HAN-ts (O), MeHAN-ts NO → N), and MeHAN-ts (O) optimized at the B3LYP/6-311++G(d,p) level. Bond lengths (Å) are given for atoms involved in hydrogen bonding. Methyl substitution on hydroxylammonia stabilizes the cation and weakens the hydrogen bonds.

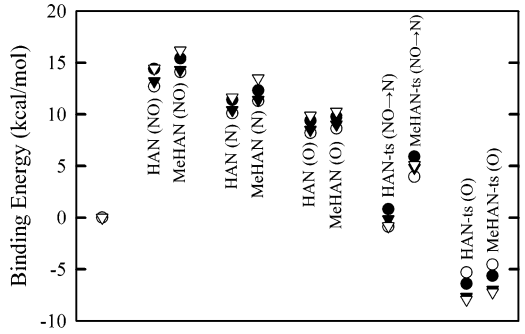

Figure 6. Binding energies D_b^{NCP} (●) from DFT calculations and D_0^{NCP}(O), D_b^{CP}(▼), and D_b^{NCP}(▽) from MP2 calculations of HAN and MHAN configurations along with the proton-transfer transition states. The structures of the molecules and transition states are given in Figures 4 and 5.

complexes for substituted and unsubstituted ammonia groups. The stronger binding is reflected in the properties of the H−O bond in the nitric acid portion of the complex and in the N···H hydrogen bond lengths. The nitric acid O−H bond length, r_{OH}, and stretch frequency, ν_{OH}^{s}, and the N···H bond lengths in the A−H···B molecules are given in Table 3. In all cases, hydrogen bonding weakens the O−H bond as manifested by an increase in the O−H bond length and the red shift in the O−H stretch frequency compared to those of gas-phase nitric acid. There is a lengthening of the bonds between ∼2 to ∼9% and red shifts from ∼300 to ∼1400 cm^{-1} in going from free gas-phase $H-ONO_2$ to the hydrogen-bonded $O_2NO-H\cdots NH_3$ complex. When a single alkyl substitution is made on the ammonia, increases of about 2% in bond length and 300 cm^{-1} in frequency are observed relative to that of the unsubstituted salt. These values are obtained by comparing the bond lengths and

TABLE 3: H−O Bond Lengths (Å), Unscaled Vibrational Stretch Frequencies (cm^{-1}), and N···H Hydrogen-Bond Distances (Å) of Nitric Acid and the Neutral Gas-Phase Hydrogen-Bonded Ammonium Salt Molecules Calculated at the B3LYP/6-311++G(d,p) Level

molecule	r_{OH}	ν_{OH}^{s}	$r_{N\cdots H}$
$HONO_2$	0.972	3550	
$NH_3\cdots HONO_2$	1.0251	2730	1.663
$CH_3NH_2\cdots HONO_2$	1.0429	2435	1.600
$C_2H_5NH_2\cdots HONO_2$	1.0440	2418	1.598
$(CH_3)_2NH\cdots HONO_2$	1.0616	2151	1.547
HAN (NO-bonded)	1.0292	2653	1.652
HAN (N-bonded)	1.0168	2864	1.699
HAN (O-bonded)	0.9961	3258	1.697
MeHAN (NO-bonded)	1.0470	2364	1.591
MeHAN (N-bonded)	1.0298	2638	1.644
MeHAN (O-bonded)	0.9974	3232	1.691

frequencies of MeAN and EtAN with AN, MeHAN (NO-bonded) with HAN (NO-bonded), and MeHAN (N-bonded) with HAN (N-bonded). The methyl and ethyl substitutents have very similar effects on the O−H bond length and frequencies. If the methyl group is located one bond away from the hydrogen-bonding atom, then its effects on the bond lengths and stretch frequencies are diminished. Note the almost identical values of the bond lengths and vibrational frequencies of HAN (O-bonded) (0.996 Å and 3258 cm^{-1}) and MeHAN (O-bonded) (0.997 Å and 3232 cm^{-1}). The alkyl group is too far removed from the oxygen atom of hydroxylammonium to contribute charge and thus stabilize the hydrogen bond. The dimethyl-substituted ammonia in diMeAN produces an even longer OH bond (1.0616 Å) and a frequency-shift difference of ∼600 cm^{-1} (actual frequency, 2151 cm^{-1}) compared to AN, for which the corresponding values are 1.0251 Å and 2730 cm^{-1}. Parallel to the increase of the H−O bond length, the H···N bond length decreases in the alkyl-substituted molecules, indicating a strengthening of the hydrogen bonds.

The alkyl substituents significantly stabilize the $A^-\cdots H-B^+$ ion-pair transition-state structures. A single alkyl substitution at the site of the hydrogen-bonding N atom increases the binding energy in the range of 5 to 6 kcal/mol. This is seen by comparing the D_b values given in Table 2 for AN-ts with those of MeAN-ts and EtAN-ts and also HAN-ts (NO → N) with MeHAN-ts (NO → N). Once again, because the site of substitution in MeHAN-ts(O) is removed from the hydrogen bonding, the binding energies of HAN-ts (O) and MeHAN-ts (O) are similar. The transition state for the dialkylamine (diMeAN-ts) has a binding energy that is ∼8 kcal/mol greater than that for AN-ts. As seen in Figures 2 and 4, the length of the H···O hydrogen bond in the transition-state complexes increases with alkyl substitution. This shows that the hydrogen bonds in the alkyl-substituted transition states are weaker than in the unsubstituted cases,that is, AN-ts or HAN-ts. The greater stability of the transition states in the alkyl-substituted cases is thus not related to the strength of the intermolecular hydrogen bonds.

An approximate measure of the magnitude of Coulombic interactions between the acid and base components in the neutral- and ion-pair complexes can be obtained by calculating the electrostatic interactions between point charges located on the nuclei of two different molecules. This electrostatic interaction energy, E_{coul}, is given by

$$E_{coul} = \sum_{i,j} \frac{q_i q_j}{4\pi\epsilon_0 r_{ij}} \qquad (7)$$

where r_{ij} is the separation between atoms i and j that are on

TABLE 4: Proton Affinity as Defined in Equation 8

	proton affinity			
molecule	B3LYP (ZPE)[a]	MP2[b]	experiment	high-level theory
$NH_3 + H^+ \rightarrow NH_4^+$	211.8 (202.3)	213.4	204.0[c]	
$CH_3NH_2 + H^+ \rightarrow CH_3NH_3^+$	222.8 (213.2)	224.0	214.9[c]	
$C_2H_5NH_2 + H^+ \rightarrow C_2H_5NH_3^+$	226.2 (216.7)	226.5	218.0[c]	
$(CH_3)_2NH + H^+ \rightarrow (CH_3)_2NH_2^+$	230.0 (220.1)	231.2	222.0[c]	
$H_2NOH + H^+ \rightarrow H_2N^+OH_2$	200.5 (191.7)	202.0	193.7[d]	
$CH_3NHOH + H^+ \rightarrow CH_3N^+H_2OH$	211.5 (202.4)	212.7	205.1[d]	
$H_2NOH + H^+ \rightarrow H_3NO^+H$	174.8 (167.2)	175.2		167.4[e]
$CH_3NHOH + H^+ \rightarrow CH_3NHO^+H_2$	182.6 (175.6)	180.5		175.1[e]

[a] Calculations at the B3LYP/6-311++G(d,p) level. Zero-point energy corrected values in parentheses. [b] Calculations at the MP2/6-311++G(d,p)// B3LYP/6-311++G(d,p) level. [c] Experimental data from the NIST database[40]. [d] Experimental data from mass spectrometric measurements, Angelelli et al.[41] [e] From G1 method calculations, Angelelli et al.[41]

TABLE 5: Reaction Energies (kcal/mol) for Proton Transfer between the Neutral and Ionic Forms of Ammonium and Alkylated Ammonium Salts

molecule	$\Delta E_r^{NCP\ a,b}$	$\Delta E_{r0}^{NCP\ a,b,c}$	$\Delta E_r^{CP\ a,d}$	$\Delta E_r^{NCP\ b,e}$
$NH_3\cdots HNO_3 \rightarrow NH_4+ \cdots NO_3^-$	8.1	7.9	7.6	11.1
$CH_3NH_2\cdots HNO_3 \rightarrow CH_3NH_3^+\cdots NO_3^-$	4.1	4.4	3.6	6.7
$C_2H_5NH_2\cdots HNO_3 \rightarrow C_2H_5NH_3^+\cdots NO_3^-$	3.7	3.1	3.3	6.4
$(CH_3)_2NH\cdots HNO_3 \rightarrow (CH_3)_2NH_2^+ \cdots NO_3^-$	1.4	2.3	0.6	3.7
HAN (NO-bond) → HAN-ts (NO→N)	13.6	13.6	13.4	15.2
MeHAN (NO-bond) → MeHAN-ts (NO→N)	9.5	10.1	9.5	11.1
HAN (O-bonded) → HAN-ts (O)	15.8	13.5	16.2	17.8
MeHAN (O-bonded) → MeHAN-ts (O)	15.4	13.2	16.0	17.5

[a] Calculations at the B3LYP/6-311++G(d,p) level. [b] Counterpoise corrections are not included. [c] Includes zero-point energies. [d] Includes counterpoise corrections. [e] Calculations at the MP2/6-311++G(d,p)// B3LYP/6-311++G(d,p) level.

different molecules, q_i and q_j are the partial charges on the atoms, and ϵ_0 is the dielectric permittivity constant for vacuum; the summation is over only the intermolecular distances. Using the interatomic separations obtained from the DFT geometry optimizations and the values of the charges from natural population analysis (NPA),[40] we can calculate the electrostatic interaction energy for the neutral- and ion-pair species. These values are given in the last column of Table 2. Because NPA charges give only approximate measures of the continuous electrostatic charge distribution in the molecules, the absolute values calculated with eq 7 are not directly comparable to the binding energies of the fragments determined from ab initio calculations. However, the values of the electrostatic energy in Table 2 are expected to be qualitatively accurate, and thus it is informative to examine the trends in them.

Alkyl substitutions generally increase the electrostatic interactions in the neutral-pair hydrogen-bonded complexes. (See column 6 of Table 2.) For example, E_{coul} increases from −16.1 kcal/mol in AN to −17.3 and −19.6 kcal/mol in MeAN and diMeAN, respectively. However, because of the dispersion of the electrostatic charge in the alkylated molecules, the magnitude of the electrostatic interaction decreases in the ion-pair transition states of the alkylated species compared to those of the nonalkylated species. For example, E_{coul} decreases from −92.8 kcal/mol in AN-ts to −92.1 and −71.4 kcal/mol in MeAN-ts and diMeAN-ts, respectively.

The main contributing factor to the stability of the alkyl-substituted ion-pair transition states is the proton affinity, PA, of the base species. For a base :B, the proton affinity is defined as

$$:B + H^+ \rightarrow H{-}B^+ \qquad PA \equiv -\Delta E \tag{8}$$

The values of PA are given in Table 4. Experimental[41,42] and high-level theoretical values[42] are given in the last column of Table 4. The agreement between the DFT proton affinities, with zero-point energy corrections included, and the experimental and high-level theoretical values is excellent.

A comparison of the proton affinity of NH_3 with that of CH_3NH_3 and $C_2H_5NH_2$ shows that a single alkyl substitution at the basic nitrogen site increases the proton affinity by ∼11 kcal/mol. The proton affinity of the doubly substituted dimethylamine is ∼18 kcal/mol higher than that of ammonia, whereas the proton affinity of trimethylamine ($(CH_3)_3NH$) is 226.8 kcal/mol,[41] which is ∼23 kcal/mol higher than that of ammonia. The proton affinity gives a measure of the basicity of the molecule. These values are in good accord with the well-known rule from organic chemistry that the electron-donating inductive effect of alkyl groups stabilizes the positive charge on the atom to which they are bound and thus increases the basicity of the substance. The larger proton affinity of the substituted bases stabilizes the positive charge of the $A^-\cdots H{-}B^+$ complexes with substituted ammonium groups compared to those with unsubstituted ammonium.

We now consider the effects on proton transfer of OH substitution on nitrogen by comparing NH_3 with NH_2OH and CH_3NH_2 with CH_3NHOH. The computed values of the PA for NH_3 and NH_2OH are 211.8 and 200.5 kcal/mol, respectively, and the values for CH_3NH_2 and CH_3NHOH are 222.8 and 211.5 kcal/mol. These values show that an OH substitution at the nitrogen site decreases the proton affinity of the nitrogen atom by ∼10 kcal/mol. The smaller proton affinities of the hydroxyl-substituted amines are one of the factors contributing to the low stability of their transition states.

The effects of the alkyl substitutions on the reaction energy of $A{-}H\cdots:B \rightarrow A^+\cdots H{-}B^-$ are illustrated by the results given in Table 5. Alkyl substitutions significantly diminish the energy barrier of this reaction. For example, compare the reaction energy of

$$H_3N\cdots HONO_2 \rightarrow NH_4^+\cdots NO_3^- \tag{9}$$

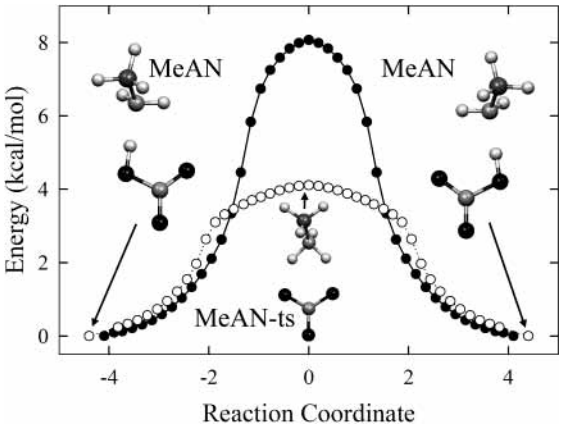

Figure 7. Energy barrier to proton exchange as a function of the reaction coordinate for AN (●) and MeAN (O) from B3LYP/6-311++G(d,p) calculations. The transition-state barrier is reduced by ~4 kcal/mol with a methyl substitution. The width of the transition-state barriers is seen to increase with the mass of the substituted alkyl groups. This is an indication of the effect of heavy-atom motion on the proton-transfer process.

to that of

$$(CH_3)_2HN\cdots HONO_2 \rightarrow (CH_3)_2NH_2^+\cdots NO_3^- \qquad (10)$$

At the noncounterpoise MP2 level, the reaction energy of eq 9 is 11.1 kcal/mol but only 3.7 kcal/mol for eq 10. The inclusion of zero-point energy and counterpoise corrections changes these values by 1 to 2 kcal/mol. This drop in proton-transfer energy facilitates the formation of the ion-pair transition state, and as a result, proton-exchange reactions can occur at lower temperatures for alkyl-substituted ammonia molecules. A comparison of the ΔE_r^{NCP} values in Table 5 shows that DFT predicts lower transition-state barriers than MP2. This is consistent with the observations made for proton-transfer barriers in other hydrogen-bonded systems.[31−33]

Alkyl substitutions also change the reaction profile for proton transfer. The reaction profiles of proton transfer and proton exchange (double proton transfer) in AN and MeAN are shown in Figure 7. Although the proton-transfer barrier is lower, the width is greater in MeAN than in AN. Proton transfer involves considerable heavy-atom motion that affects the width of the reaction barrier. The greater the mass and the more concerted the motions of the heavy atoms that are coupled to the proton transfer, the wider the barrier. The extent of heavy-atom motion involved in the proton transfer can be seen by comparing the N···N distances in the neutral-pair and ion-pair species. Values for the these distances are given in Figures 1 and 2. The N···N distances for AN, MeAN, EtAN, and diMeAN are 3.359, 3.322, 3.325, and 3.287 Å, respectively. (See Figure 1.) This distance becomes shorter as the hydrogen-bond strength increases from AN to diMeAN. The N···N distances for the AN-ts, MeAN-ts, EtAN-ts, and diMeAN-ts species are 2.990, 3.022, 3.032, and 3.049 Å, respectively. (See Figure 2.) This distance increases as the hydrogen-bond strength decreases from AN-ts to diMeAN-ts. The extent of heavy-atom motion in proton transfer decreases for the progression from AN → AN-ts to diMeAN → diMeAN-ts.

V. Summary and Conclusions

The binding energies of the nitrate salts of ammonia, methylamine, ethylamine, dimethylamine, hydroxylamine, and methylhydroxylamine have been studied at the B3LYP/6-311++G(d,p) level of theory. Zero-point energy and counterpoise corrections have been applied to these values. Single-point energy determinations at the MP2/6-311++G(d,p)//B3LYP/6-311++G(d,p) level verify the qualitative aspects of our DFT calculations. The main conclusions of this work are the following:

·Alkyl substitutions increase the binding strengths of both neutral-pair and ion-pair complexes.

·Alkyl substitutions stabilize the ion-pair complexes to a greater extent than the neutral pairs.

·The activation barrier for proton transfer from the neutral pair to form the ion pair is decreased as a result of alkyl substitutions.

·The effect of the alkyl substituents may be analyzed in terms of electrostatic interactions, hydrogen-bond strengths, and proton affinities. The stability of the alkyl-substituted complexes is mainly due to the increased proton affinity of the substituted base. The electrostatic interactions and hydrogen bonding are actually weakened by the presence of an alkyl group on the nitrogen.

References and Notes

(1) Scheiner, S. *Hydrogen Bonding. A Theoretical Perspective*; Oxford University Press: Oxford, U.K., 1997.

(2) Jeffery, G. A. *An Introduction to Hydrogen Bonding*; Oxford University Press: Oxford, U.K., 1997.

(3) Lanyi, J. K. *J. Biol. Chem.* **1997**, *272*, 31209.

(4) Krasnogholovets, V. V.; Taranenko, V. B.; Tomchuk, P. M.; Protsenko, M. A. *J. Mol. Struct.* **1997**, *355*, 219.

(5) Krasnoholovets, V. V.; Tomchuk, P. M.; Lukyanets, S. P. In *Advances in Chemical Physics*; Prigogine, I., Rice, S. A., Eds.; Vol. 125; Wiley: New York, 2003.

(6) Michel, H. *Proc. Natl. Acad. Sci. U.S.A.* **1998**, *95*, 12819.

(7) Gennis, R. B. *Proc. Natl. Acad. Sci. U.S.A.* **1998**, *95*, 12747.

(8) Brill, T. B.; Bundez, B. T. In *Solid Propellant Chemistry, Combustion and Motor Interior Ballistics*; Yang, V., Brill, T. B., Ren, W.-Z., Eds.; Progress in Astronautics and Aeronautics, Vol. 185; American Institute of Aeronautics and Astronautics: Reston, VA, 2000; pp 3−32.

(9) Nguyen, M.-T.; Jamka, A. J.; Cazar, R. A.; Tao, F.-M. *J. Chem. Phys.* **1997**, *106*, 8710.

(10) Tao, F.-M. *J. Chem. Phys.* **1998**, *108*, 193.

(11) Alavi, S.; Thompson, D. L. *J. Chem. Phys.* **2002**, *117*, 2599.

(12) Rossi, M. J.; Bottaro, J. C.; McMillen, D. F. *Int. J. Chem. Kinet.* **1993**, *25*, 549.

(13) Alavi, S.; Thompson, D. L. *J. Chem. Phys.* **2003**, *118*, 2599.

(14) Alavi, S.; Thompson, D. L. *J. Chem. Phys.* **2003**, *119*, 4274.

(15) Meuwly, M.; Karplus, M. *J. Chem. Phys.* **2002**, *116*, 2572.

(16) Schoeder, O. E.; Andriole, E. J.; Carver, K. L.; Colyer, K. E.; Poutsma, J. C. *J. Phys. Chem. A* **2004**, *108*, 326.

(17) Alkorta, I.; Elguero, J. *J. Phys. Chem. A* **2002**, *103*, 117.

(18) Alkorta, I.; Rozas, I.; Mó, O.; Yáñez, M.; Elguero, J. *J. Phys. Chem. A* **2001**, *105*, 7481.

(19) Legon, A. C.; Rego, C. A. *J. Chem. Phys.* **1989**, *90*, 6867.

(20) Legon, A. C.; Wallwork, A. L.; Rego, C. A. *J. Chem. Phys.* **1990**, *92*, 6397.

(21) Legon, A. C.; Rego, C. A. *J. Chem. Phys.* **1993**, *99*, 1463.

(22) Barnes, A. J.; Legon, A. C. *J. Mol. Struct.* **1998**, *448*, 101.

(23) Legon, A. C. *Chem. Soc. Rev.* **1993**, *22*, 153.

(24) Latajka, Z.; Scheiner, S.; Ratajczak, H. *Chem. Phys.* **1992**, *166*, 85.

(25) Frisch, M. J.; Trucks, G. W.; Schlegel, H. B.; Scuseria, G. E.; Robb, M. A.; Cheeseman, J. R.; Zakrzewski, V. G.; Montgomery, J. A., Jr.; Stratmann, R. E.; Burant, J. C.; Dapprich, S.; Millam, J. M.; Daniels, A. D.; Kudin, K. N.; Strain, M. C.; Farkas, O.; Tomasi, J.; Barone, V.; Cossi, M.; Cammi, R.; Mennucci, B.; Pomelli, C.; Adamo, C.; Clifford, S.; Ochterski, J.; Petersson, G. A.; Ayala, P. Y.; Cui, Q.; Morokuma, K.; Malick, D. K.; Rabuck, A. D.; Raghavachari, K.; Foresman, J. B.; Cioslowski, J.; Ortiz, J. V.; Stefanov, B. B.; Liu, G.; Liashenko, A.; Piskorz, P.; Komaromi, I.; Gomperts, R.; Martin, R. L.; Fox, D. J.; Keith, T.; Al-Laham, M. A.; Peng, C. Y.; Nanayakkara, A.; Gonzalez, C.; Challacombe, M.; Gill, P. M. W.; Johnson, B. G.; Chen, W.; Wong, M. W.; Andres, J. L.; Head-Gordon, M.; Replogle, E. S.; Pople, J. A. *Gaussian 98*, revision A.7; Gaussian, Inc.: Pittsburgh, PA, 1998.

(26) Parr, R. G.; Yang, W. *Density Functional Theory of Atoms and Molecules*; Oxford University Press: New York, 1989.

(27) Koch, W.; Holthausen, M. C. *A Chemist's View of Density Functional Theory*; Wiley-VCH: Weinheim, Germany, 2000.
(28) Becke, A. D. *J. Chem. Phys.* **1993**, *98*, 5648.
(29) Sadhukhan, S.; Munoz, D.; Adamo, C.; Scuseria, G. E. *Chem. Phys. Lett.* **1999**, *306*, 83.
(30) Pavese, M.; Chawla, S.; Lu, D.; Lobaugh, J.; Voth, G. A. *J. Chem. Phys.* **1997**, *107*, 7428.
(31) Meuwly, M.; Bach, A.; Leutwyler, S. *J. Am. Chem. Soc.* **2001**, *123*, 11446.
(32) Møller, C. M.; Plesset, M. S. *Phys. Rev.* **1934**, *46*, 618.
(33) Pople, J. A.; Binkely, J. S.; Seeger, R. *Int. J. Quantum Chem.* **1976**, *10*, 1.
(34) Mebel, A. M.; Morokuma, K.; Lin, M. C. *J. Chem. Phys.* **1995**, *103*, 7414.
(35) Levine, I. N. *Quantum Chemistry*; Prentice Hall: Englewood Hills, NJ, 1991.
(36) Tao, F.-M. *Int. Rev. Phys. Chem.* **2001**, *20*, 617.
(37) Boys, S. F.; Bernardi, F. *Chem. Phys.* **1970**, *232*, 299.
(38) Xantheas, S. S. *J. Chem. Phys.* **1996**, *104*, 8821.
(39) Zhang, Q.; Bell, R.; Truong, T. N. *J. Phys. Chem.* **1994**, *99*, 592.
(40) Glendening, E. D.; Reed, A. E.; Carpenter, J. E.; Weinhold, F. *NBO*, version 3.1. Reed, A. E.; Weinhold, F. *J. Am. Chem. Soc.* **1980**, *102*, 7211. Reed, A. E.; Curtiss, L. A.; Weinhold, F. *Chem. Rev.* **1988**, *88*, 899.
(41) NIST Chemistry Webbook (NIST Standard Reference Database No. 69, March 2003 release) www.nist.org.
(42) Angelelli, F.; Aschi, M.; Cacace, F.; Pepi, F.; de Petris, G. *J. Phys. Chem.* **1995**, *99*, 6551.